

John H. Root

e-mail: John.Root@nrc.ca

J. Katsaras

e-mail: John.Katsaras@nrc.ca

National Research Council of Canada,
Chalk River Laboratories,
Chalk River, Ontario, Canada K0J 1J0

John F. Porter

Defense Research Establishment Atlantic,
HMC Dockyard,
Halifax, Nova Scotia, Canada B3K 2X0
e-mail: Porter@drea.dnd.ca

Brian W. Leitch

Atomic Energy of Canada Limited,
Chalk River Laboratories,
Chalk River, Ontario, Canada K0J 1J0
e-mail: Leitchb@aecl.ca

Neutron Diffraction Maps of Stress Concentration Near Notches Under Load at Temperature

Recent advances in neutron detector technology and the ability of neutrons to penetrate through many millimeters of most engineering materials have made it feasible to investigate the effects of sub-surface stress-concentration in the vicinity of notches. Neutron-diffraction strain measurements are non-destructive and capable of tracking the development of the elastic strain field as a function of applied load in a single specimen. This paper presents two demonstrations of neutron-diffraction strain-scanning with high spatial resolution. First, the development of the strain field near a notch in an HY-100 steel bar is scanned as a three-point bending load is increased to the point of metal-tearing. Second, the stress-concentration effects of a blunt notch in a tensile test specimen are presented. The measurements are performed while the specimen is held at a temperature of 250°C and while load is applied to maintain constant total strain. The neutron diffraction measurements reveal a gradual redistribution of the stress concentration over time. In both examples, the gradients of the strain distribution are substantial, but neutron diffraction has a sufficient spatial resolution (of the order 0.5 mm to 1.0 mm) to characterize the details of a stress concentration field. [DOI: 10.1115/1.1482407]

Introduction

Nondestructive strain measurements are made by neutron diffraction to scan the internal distribution of stresses in intact engineering components, such as bent tubes [1], welded plates [2], and welded pipes [3]. Because it is nondestructive, the neutron-diffraction strain-scanning technique can track the development of the elastic strain field in a single specimen as applied load is increased. Neutron beams can also penetrate through heating elements to scan the strain distribution in specimens that are held at some temperature that is characteristic of in-service conditions.

By characterizing the effects of load and temperature on internal stress distributions, one may begin to address fundamental issues of the fitness-for-service of critical engineering components [4]. For this paper, a notched bar of HY-100 steel was subjected to three-point bending to the point of metal tearing and neutron diffraction traced the evolution of the strain distribution near the notch. The HY-100 material is found in marine structures, where a robust response to plastic deformation and crack formation is needed. Also for this paper, neutron diffraction scans were made of the strain distribution below a semi-circular groove in a tensile specimen of Zr-2.5Nb, held at a temperature of 250°C. This experiment begins to investigate the possible relaxation of stress-concentration effects of fretting flaws or corrosion pits that might appear in pressurized piping systems.

Incident and diffracted neutron beams intersect to form a small "sampling volume" that is scanned through a raster of locations inside a component. At each location, a diffraction peak is acquired, the mean scattering angle (2θ) is determined, and the crystal-lattice strain, ε , is determined by comparison with the scattering angle for stress-free material ($2\theta_o$), through the relation

$$\varepsilon = \frac{\sin \theta_o}{\sin \theta} - 1 \quad (1)$$

Contributed by the Pressure Vessels and Piping Division and presented at the Pressure Vessels and Piping Conference, Atlanta, Georgia, July 22–26, 2001, of THE AMERICAN SOCIETY OF MECHANICAL ENGINEERS. Manuscript received by the PVP Division, December 19, 2000; revised manuscript received March 29, 2002. Associate Editor: S. Y. Zamrik.

Unlike a mechanical strain gage, which measures total strain, this crystal-lattice strain is purely elastic, reflecting the stresses in crystallites, and is not directly sensitive to plastic strain.

Typical incident neutron beam fluxes lie in the range of $(0.5-5) \times 10^4$ neutrons/mm²/s. Diffraction from randomly-oriented polycrystalline materials in a sampling volume of the order 1 mm³, yields detected-neutron intensities on the order of 0.1–10 counts per second. The challenge in neutron diffraction-based strain scanning is to optimize the rate at which data can be collected while retaining a sufficient spatial resolution to characterize stress-gradients adequately. These stress gradients are particularly steep when approaching stress-concentrators. For example a thin plate, deformed elastically, has an intensified stress that increases by a factor of $1/r^{1/2}$ as the distance to a notch tip, r , is reduced [5].

In-Situ Neutron Diffraction

The L3 neutron diffractometer (Fig. 1) is situated at the NRU reactor, a medium-flux source of thermal neutrons, located at Chalk River Laboratories in Canada. The diffractometer is equipped with a 32-element multiwire ³He detector that spans 2.7 deg in 2θ , and can acquire a complete diffraction peak in one setting. The incident and diffracted neutron beams were defined by slits in neutron-absorbing cadmium masks. Slit dimensions were chosen as a best compromise between spatial resolution and signal intensity for each experiment. The specimen table on the diffractometer is equipped with computer-controlled XYZ translators that can handle loads up to 500 kg.

To apply three-point bending loads to the notched HY-100 bar, a screw-driven clamp, which weighed more than 100 kg, was attached to the translator so the specimen-plus-clamp could be positioned during strain scanning.

Tensile loads were applied to the Zr-2.5Nb specimen by a universal testing machine with a capacity of 50 kN [6]. The testing machine was also mounted on the translator system for scanning of strain within the loaded specimen.

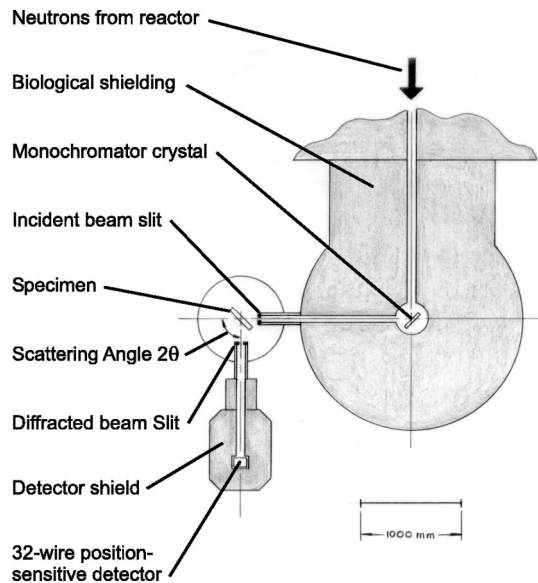


Fig. 1 Sketch of L3 neutron diffractometer

HY-100 Notched Bar in Three-Point Bending

Experimental Details. A sketch of the three-point bending specimen is shown in Fig. 2. The bar was about 16 mm thick, 38 mm in the vertical direction and 220 mm in the longitudinal direction. The bar was oriented such that the longitudinal component of strain was measured. The bending loads were applied in the vertical direction through large-diameter pins. An overall measure of distortion was monitored by a strain gage attached to the bottom surface of the bar. Strains were determined from shifts in 2θ of the (110) diffraction peak from the body-centered cubic crystal structure of the HY-100 steel. The stress-free value, $2\theta_0$, was determined from measurements in the bar prior to the application of load. The sampling volume had dimensions $1.5\text{ mm} \times 1.5\text{ mm} \times 2\text{ mm}$, with the long dimension parallel to the vertical direction. The raster of measurement locations extended upwards from the root of a sharp notch and to one side. All measurements were made at mid-thickness of the bar. Strain scans were made with strain-gage readings that included 10.0×10^{-4} (mainly elastic deformation), 16.2×10^{-4} (plastic zone developing), 16.7×10^{-4} (internal crack develops), and finally 0.0 (residual stresses).

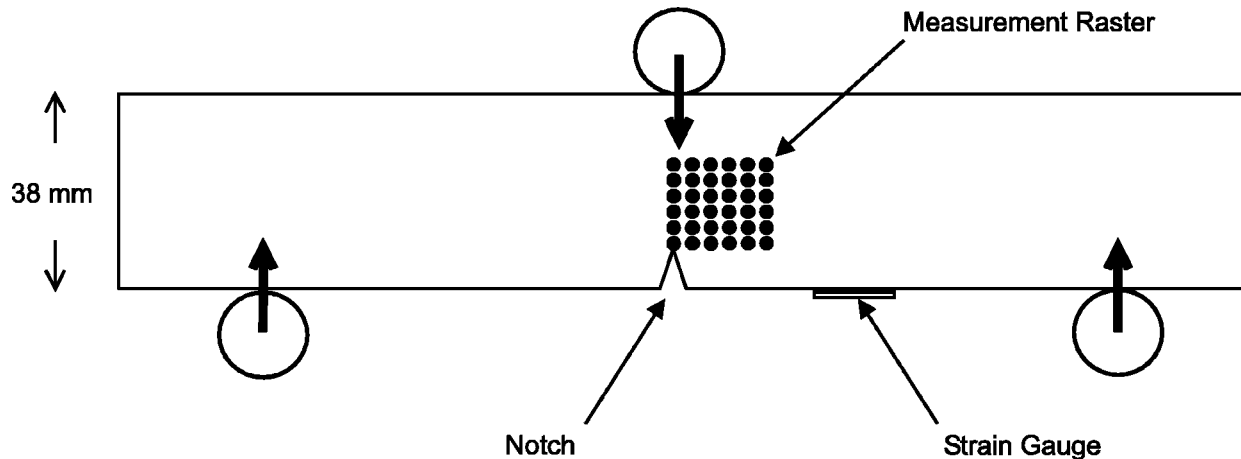


Fig. 2 Sketch of notched HY-100 bar in three-point bending configuration

Results for Various Bending Loads. Maps of the longitudinal component of strain versus distance from the original notch tip are presented in Fig. 3. Note in these plots that the maximum vertical distance from the notch tip corresponds approximately to the neutral axis of the bent bar, not to the top surface of the bar. A characteristic “butterfly” pattern of elastic strain is well-developed with low deformation of the bar (Fig. 3(a)). A maximum strain value, $+25 \times 10^{-4}$, occurs about 3 mm above the notch, but values close to this maximum extend towards the tip of the notch. On increasing the bend to a point that significant plasticity occurs (Fig. 3(b)), the maximum strain increases to about $+40 \times 10^{-4}$ and remains at the same distance from the original notch tip. This strain maximum is more localized than was observed at the lower load. On approach to the original notch tip there is a factor-of-two reduction of lattice strain, which is a consequence of plasticity near the notch. Increasing the bend still further (Fig. 3(c)), there is a dramatic shift of the strain maximum away from the original notch tip. This shifted pattern of strain, measured at mid-thickness of the bar, suggests the presence of an internal crack. The crack could not be seen at the surface of the bar, but the near-zero longitudinal strain, which appears at the location of the original notch tip, supports the idea that an internal crack was formed. (The stress normal to a crack surface is zero, and the crystal lattice strains measured in the same direction would be close to zero, as observed.) When a similar bar was bent slightly beyond the deformation indicated as 16.7×10^{-4} on the strain gage, a metal tear appeared clearly on the surface. Unloading the bar from the condition in (Fig. 3(c)), a residual strain pattern was obtained (Fig. 3(d)). Along the line directly above the notch, one observes the classic residual-strain pattern of a bent plate. This bent-plate pattern is confined closely to the line above the notch. As little as 15 mm away from this line, in the longitudinal direction, it appears as if no plastic deformation has occurred.

Evolution of Stress-Concentration Near a Blunt Notch Held at 250°C While Under Load

Experimental Details. A sketch of the Zr-2.5Nb tensile specimen is shown in Fig. 4. The specimen was 4 mm thick, 6.5 mm wide, and had a gage length of 50 mm. A semi-circular groove of radius 1 mm extended across the width of the specimen. The crystallites of the hexagonal close-packed material exhibit a preferred orientation, which enhances the signal intensity if the strain parallel to the tensile axis is determined through shifts in the scattering angle of the (0002) diffraction peak.

The temperature was maintained at $250 \pm 1^\circ\text{C}$ by a cartridge-heater assembly, which encased the gage-length of the specimen

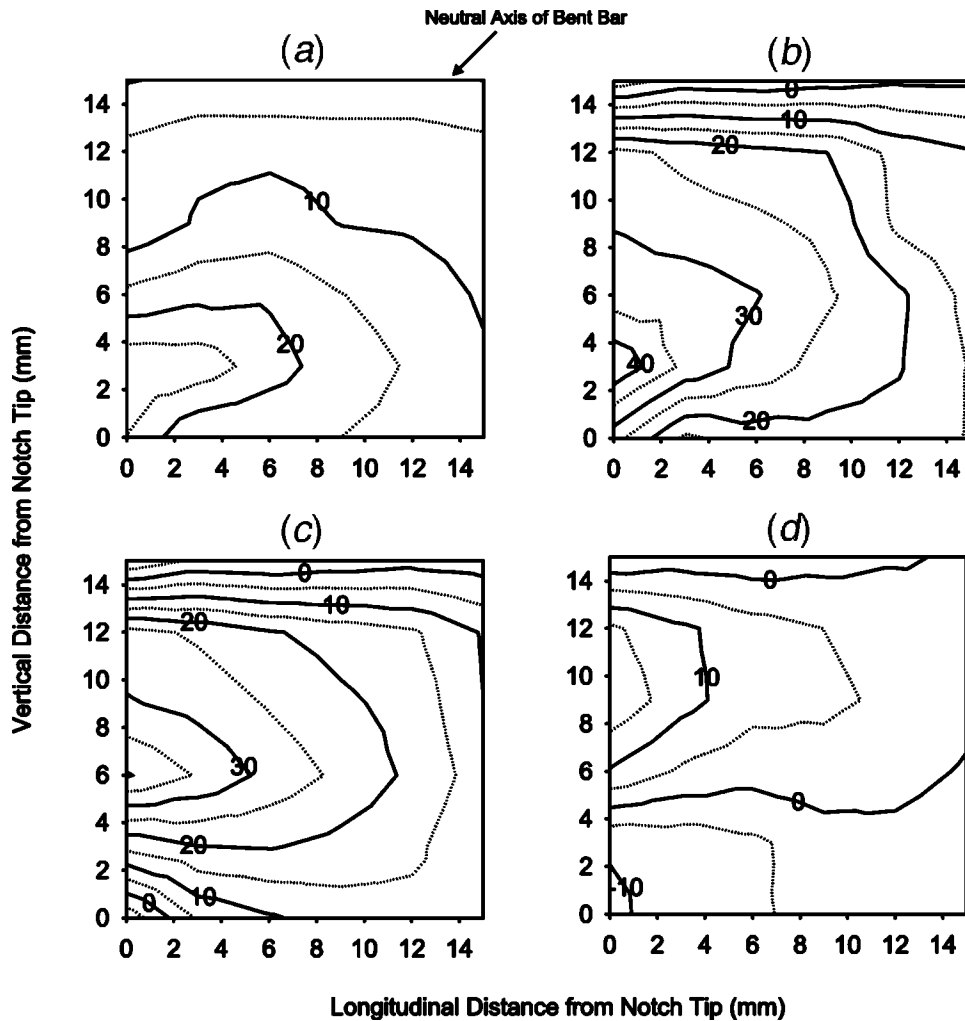


Fig. 3 Maps of longitudinal strain (10^{-4}), at various loading conditions: (a) 10×10^{-4} , (b) 16.2×10^{-4} , (c) 16.7×10^{-4} , and (d) unloaded after 16.7×10^{-4}

(Fig. 5). Temperature was monitored by a type-K thermocouple that was embedded in the heater assembly. A calibrated load cell monitored the applied load, and an extensometer monitored the total strain in the specimen, straddling the opening of the groove. The applied load was controlled to maintain a *constant total strain* (i.e., plastic strain + elastic strain = constant). The control procedure was to ramp the applied load to achieve a nominal value of stress in the gage section, $\sigma_{\text{NOM}} = 300$ MPa. At this point, the

extensometer voltage-output was read and control of the stress rig was switched to an active feedback mode where this extensometer reading was held constant. Under tensile load at 250°C , the material near the blunt notch deforms plastically, increasing the tensile plastic strain. To maintain a constant extensometer reading (i.e., a constant total strain), the applied load was gradually reduced to decrease the elastic strain.

Crystal-lattice strain scans were measured as a function of

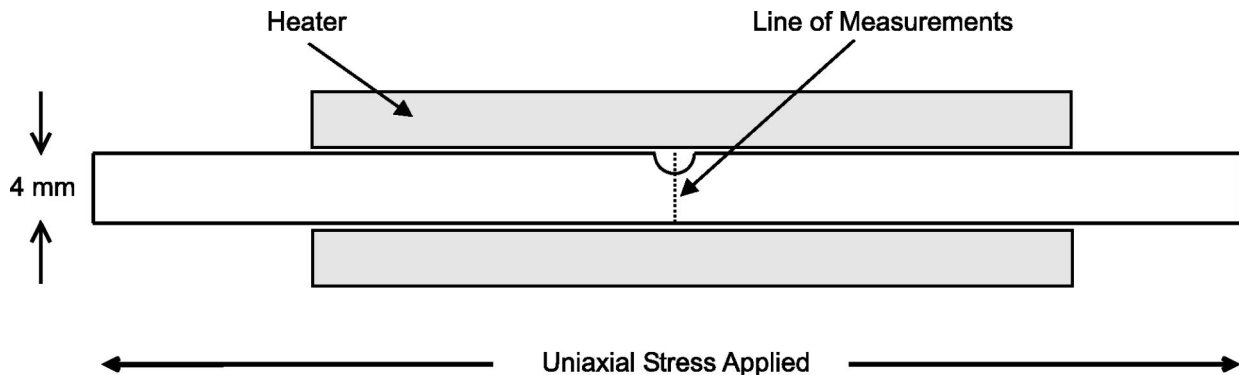


Fig. 4 Sketch of Zr-2.5Nb tensile specimen with semi-circular groove

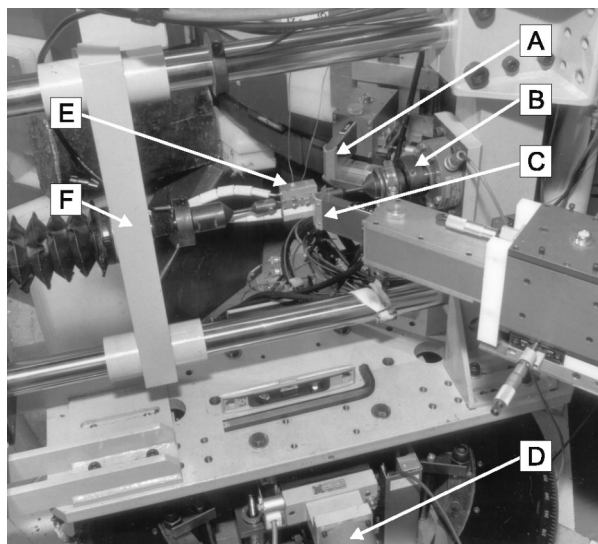


Fig. 5 Neutron diffraction apparatus: (A) incident-beam slit, (B) load cell, (C) diffracted-beam slit, (D) XYZ translators, (E) Heater, (F) screw-driven cross-head

depth below the root of the notch. The sampling volume had dimensions $0.5\text{ mm} \times 0.5\text{ mm} \times 5\text{ mm}$, with the long dimension parallel to the groove. This configuration ensured high spatial resolution of strain gradients as measurements were made along a line below the root of the groove. The scans of crystal-lattice (i.e., elastic) strain were repeated as a function of time to monitor the evolution of the stress concentration effects as plastic strain accumulated in the specimen.

Results for Tensile Loading at Temperature. The variation of elastic strain with depth below the root of the groove is presented in Fig. 6. Strain distributions are compared for times about 14 h and 87 h after the initial load was applied to the tensile specimen. The total strain, which is being maintained by the extensometer feedback loop, is shown as a reference line about which the elastic strain distribution is seen to exhibit the effects of stress concentration.

A nominal stress of 300 MPa would keep the material in the region of purely elastic response, but the blunt notch generates a stress concentration that is evident in the increased strain on approach to the root of the groove. The linear form of the strain distribution far from the notch is similar to the stress-concentration curve expected in plane-strain geometry [5]. The stress-concentration factor for this specimen geometry is about 1.7 [7]. The stresses exceed the yield point of this material as the root of the groove is approached.

The process of yielding very close to the groove happens too quickly to be captured by a time-resolved neutron diffraction experiment. The result is a turnover of the strain distribution for distances less than 1 mm from the root of the notch. It seems evident that the stress-concentration effect continues to evolve over many hours, as the load is maintained and the temperature remains at 250°C . The stress concentration pattern at 87 h is flatter than the one at 14 h, possibly indicating that the plastic zone around the groove expands with time. The plastic deformation of materials leads to a broadening of diffraction peaks. This phenomenon is complex, but has been suggested as the basis of an X-ray or neutron diffraction-based probe to evaluate the remaining life of the components that have been subjected to cyclic loads and may have accumulated some plastic damage [8]. The evolution of diffraction peak width with time is presented in Fig. 7. Results are compared for a location 1 mm below the root of the groove with a location 3 mm below the root of the groove. Closer to the groove, the diffraction peak width increases obviously with

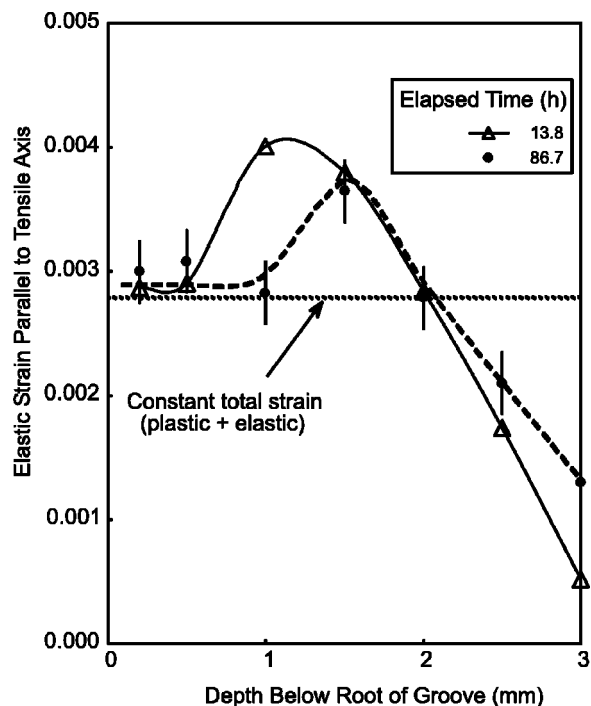


Fig. 6 Scan of crystal-lattice (elastic) strain versus depth below a blunt notch. Continuous and dashed lines are guides to the eye. Vertical bars indicate the typical measurement uncertainty $\pm \sigma$.

time, which suggests that plastic strain is accumulating. In contrast, the diffraction peak width far from the groove remains at its original low value, as might be expected if the zone of plasticity has not yet reached a distance of 3 mm from the root of the groove.

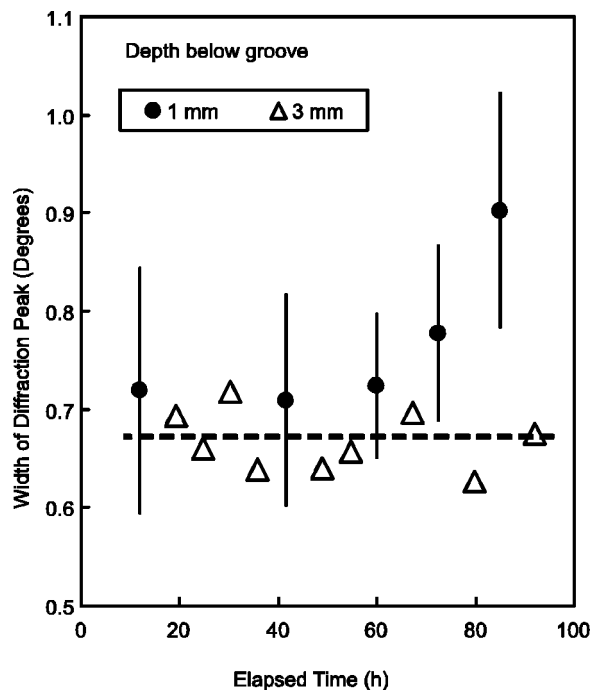


Fig. 7 Peak broadening with time. Width is the Full-Width of a diffraction peak at half of its maximum height. Vertical bars indicate the typical measurement uncertainty $\pm \sigma$. The dashed line shows the average peak width far from groove, at early times.

Discussion

The ability of neutron-diffraction to probe the stress/strain concentration fields created near a notch, nondestructively, is unique. Neutron diffraction can determine these fields inside actual engineering materials, subjected to thermal and structural loads, as may be applied to actual pressure vessel and piping systems. This work has demonstrated that the spatial resolution of the nondestructive scans of strain is sufficient to characterize the steep gradients arising in stress-concentration situations. Thus, neutron diffraction can survey the complex stress/strain fields that are created around cracks, notches or complex features such as nozzle/vessel intersections.

Because the measurements are nondestructive, the evolution of stress fields with time, or subsequent heat treatments, can be evaluated through a series of repeat measurements, for example, before and after shakedown has been carried out on a welded structure. Or, as shown in the present work, the evolution of stress fields with time at load, at various temperatures can be investigated. The fundamental knowledge obtained by such experiments can be applied to validate finite-element models of stress distributions, and to improve the reliability of conclusions that pertain to fitness-for-service of pressure systems. Understanding the material phase changes and the resultant fields created by various manufacturing methods and service conditions will allow us to improve our pressure vessel designs and safety factors.

Conclusions

With a medium-flux research reactor and a multi-wire detector, there is enough signal intensity to achieve the spatial resolution needed to characterize stress-concentration effects in realistic operating conditions of load and temperature.

It may be feasible, with neutron diffraction, to study the growth of the plastic zone near a stress-concentrating defect, as a function of time at conditions of interest for pressurized systems.

Acknowledgments

These challenging neutron strain-scanning projects were made possible with the skillful technical assistance of J. Fox, D. Tennant, M. Montaigne, L. McEwan, M. Potter and J. Bolduc. This work was partially supported by the CANDU Owners Group, WPIR 3214, Working Party 32.

Nomenclature

- 2θ = scattering angle at location in specimen (deg)
- $2\theta_o$ = scattering angle in stress-free material (deg)
- ε = crystal-lattice strain (mm/mm)
- r = distance from root of notch or tip of crack (mm)
- $\pm \sigma$ = uncertainty of measured quantity (one standard error)

References

- [1] Holden, T. M., Holt, R. A., Dolling, G., Powell, B. M., and Winegar, J. E., 1988, "Characterization of Residual Stresses in Bent INCOLOY-800 Tubing by Neutron Diffraction," *Metall. Trans. A*, **19A**, pp. 2207–2214.
- [2] Root, J. H., Holden, T. M., Schröder, J., Hubbard, C. R., Spooner, S., Dodson, T. A., and David, S. A., 1993, "Residual Stress Mapping in Multipass Ferritic Steel Weld," *Mater. Sci. Technol.*, **9**, pp. 754–759.
- [3] Root, J. H., Coleman, C. E., Bowden, J. W., and Hayashi, M., 1997, "Residual Stresses in Steel and Zirconium Weldments," *ASME J. Pressure Vessel Technol.*, **119**, pp. 137–141.
- [4] Leitch, B. W., and Tomé, C. N., 1995, "The bending of Incoloy-800 Tubes and the Resultant Internal Stresses," *Simulation of Materials Processing: Theory, Methods and Applications*, NUMIFORM 95, eds., Shen and Dawson, pp. 859–862.
- [5] Dieter, G. E., 1986, *Mechanical Metallurgy*, McGraw-Hill, Inc., New York, NY.
- [6] Applied Test Systems, Inc., 348 New Castle Rd., Box 1529, Butler, PA. 16003.
- [7] Peterson, R. E., 1974, *Stress Concentration Factors*, John Wiley and Sons, New York, NY.
- [8] Holden, T. M., Root, J. H., Fox, J., Porter, J. F., Pinneault, J. A. and Brauss, M. E., 1995, "Diffraction Measurements of Linewidth in Plastically Deformed and Fatigued HY-80 Materials," *ASME NDE for the Energy Industry 1995*, **13**, pp. 49–53.